13B.2 DUAL-POLARIZATION WEATHER RADAR OBSERVATIONS OF SNOW GROWTH PROCESSES

Dmitri Moisseev [1], Elena Saltikoff [2], Matti Leskinen [1]

[1]*Dep. of Physics, University of Helsinki, Helsinki, Finland*
[2]*Finnish Meteorological Institute, Helsinki, Finland*

ABSTRACT

Variability in ice particle physical properties is one of the major error causes in radar quantitative precipitation estimation in snowfall. In this study, morphological analysis of polarimetric radar observations is used to identify dominating snow growth mechanisms. It is demonstrated that polarimetric measurements can be used to identify aggregation, riming, vapour deposition growth patterns as well as regions of intense secondary ice production.

This study is based on measurements carried out by the radar during winters 2005-2009. The polarimetric radar observations are compared to vertically pointing Doppler spectral observations carried out by a University of Helsinki transportable C-band radar.

1. INTRODUCTION

Weather radar quantitative precipitation estimation in snowfall is notoriously difficult. Radar observations depend on phase, size, shape, and density of precipitating particles. The physical properties of ice precipitation are governed by growth mechanisms, i.e. water vapour deposition, aggregation and riming processes. It was observed that in case of rimed snowfall about half of ice mass flux is due to accreted supercooled liquid water (Feng and Grant (1982); Mitchell et al. (1990)). Or in other words, for the same number flux, precipitation rate for rimed ice particles is about twice the snowfall rate of unrimed particles. These observations show importance of identification of a dominating snow growth mechanism for radar quantitative precipitation estimation.

Typically, fuzzy logic polarimetric radar classification schemes (Liu and Chandrasekar, (2000); Straka et al. (2000), Lim et al. (2005)) are used to distinguish between different types of hydrometeors. Unfortunately, experience shows that polarimetric radar signatures are not very different for many types of ice particles, i.e. aggregates and rimed ice particles. This is seriously affecting the ability of dual-polarization classification to improve quantitative radar observations of snowfall.

The goal of this work is to study whether dual-polarization radar observations can be used to identify dominating snow growth mechanisms. The main difference of this study from the traditional fuzzy logic approaches, is that we are not trying to identify different types of ice particles for each radar pixel. Our approach is rather to analyze spatial behaviour of dual-polarization radar observations and link it to underlying physical processes.

Corresponding author address:

Dep. of Physics, University of Helsinki, PO Box 48, University of Helsinki, FIN-00014, Finland
e-mail: dmitri.moisseev@helsinki.fi

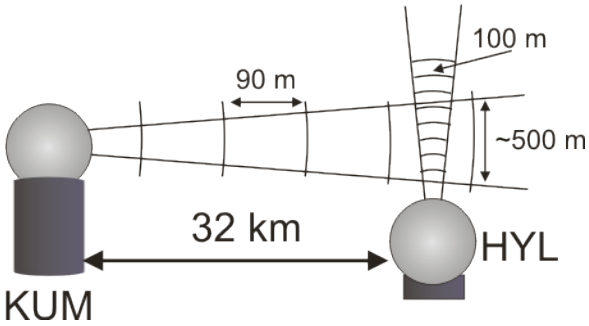

Figure 1. University of Helsinki measurement setup.

Similar to Zawadzki et al. (2001), vertically pointing Doppler radar was used to identify cases where riming was present. By carrying out a joint analysis of polarimetric and vertically pointing Doppler radar measurements, signatures that are corresponding to aggregation, riming, vapour deposition and secondary ice production were identified. The proposed morphological analysis is then was used to explain differences in snow packing, ratio of snow depth change to accumulated liquid water equivalent, for four snowfall events that took place in 2005 and 2009 in the greater Helsinki area.

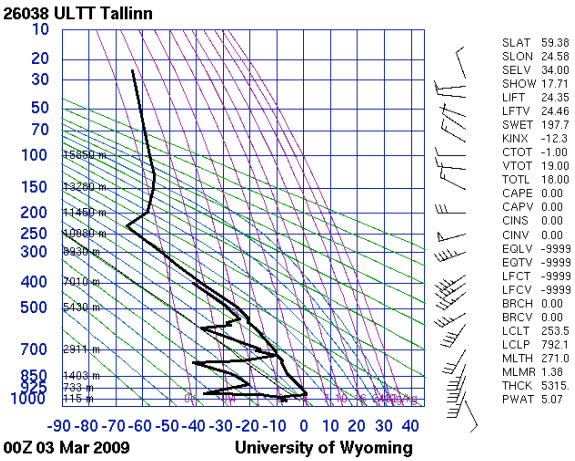

Figure 2 Tallinn sounding from 0 UTC taken on March 3rd, 2009. Sounding indicates presence of three cloud layers at 300m, 2700m and 5000 m.

2. MEASUREMENT SETUP

In Figure 1 the measurement setup used in this study is shown. University of Helsinki Kumpula radar (KUM) is a C-band polarimetric weather radar located at the top of the Department of Physics building. The radar is positioned 59 m above the mean sea level and 30 m above the ground level.

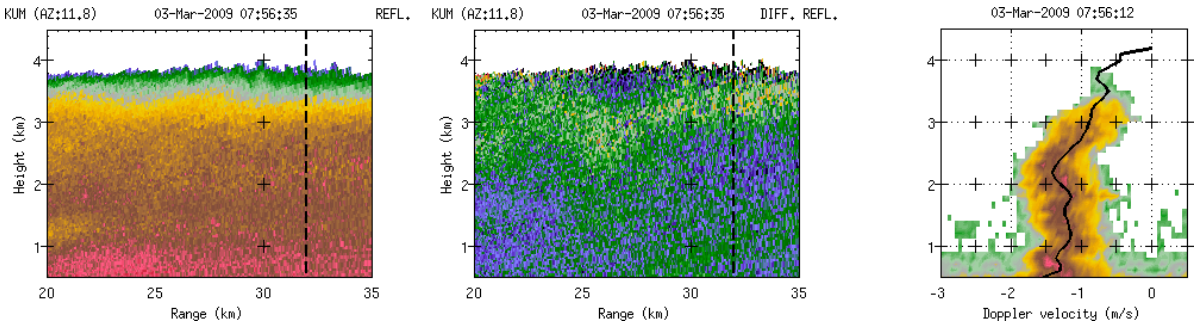

Figure 3 Radar measurements taken on March 3rd, 2009. On left two panels segments of RHI observations of reflectivity and differential reflectivity are shown. On the right panel vertically pointing Doppler spectral observations are shown. The spectral measurements were using transportable University of Helsinki radar. The location of the radar is shown by dashed line on the RHI plots.

The transportable C-band weather radar (HYL) used in this study is stationed 32 km North (azimuth 11.8 degrees) of Kumpula radar. There is a clear line of sight between the radars.

Data collected in snowfall events that took place during years 2005-2009 was used in this work. For most of the measurements transportable radar was

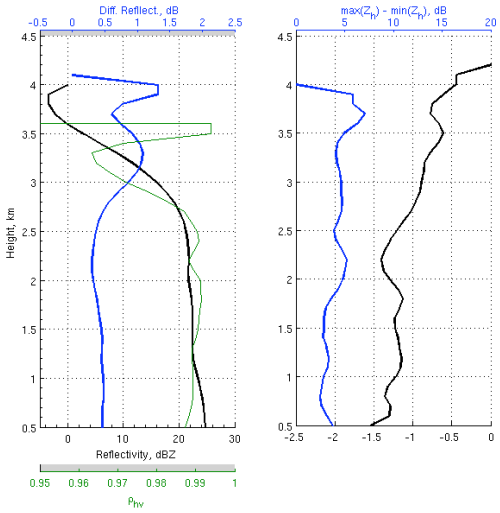

Figure 4 Coinciding profiles of reflectivity, differential reflectivity, co-pol correlation coefficient (left figure) and mean vertical velocity, span of reflectivity values (right figure) taken from the measurements shown in Figure 3. Span of reflectivity values calculated as difference of maximum and minimum reflectivity values found in the range interval 29 to 35 km for each height bin.

operating in Doppler spectral mode with antenna pointing to the zenith. Doppler spectra were collected every 10 s. At the same time, Kumpula radar was performing RHI scans over HYL radar. These scans were repeated every two minutes.

3. MEASUREMENT ANALYSIS

Lo and Passarelli (1986) have observed that there is often a little amount of liquid water present in atmosphere even when temperatures are below freezing. Depending on amount of water and droplets sizes, different growth mechanisms would dominate. Hogan et al. (2002) have shown that high differential reflectivity values can often be observed at the top or even in the middle of an ice cloud. By comparing to aircraft data the authors have concluded that those high Z_{dr} values correspond to areas where supercooled liquid water was present. They also have shown that there is an anti-correlation between reflectivity and differential reflectivity, i.e. higher Z_{dr} values correspond to lower reflectivity values. It is not quit clear though, why this apparent anti-correlation exists.

If supercooled water droplets are present inside of an ice cloud or precipitation, there are a number of processes that can manifest themselves as high Z_{dr} radar observations. Those processes are:

- Water vapor deposition growth of ice crystals
- Splinter formation during riming of ice crystals
- Enhanced ice nucleation in regions of spuriously high super saturations in the presence of large quantities of supercooled drops.

Regardless of a process that takes place inside of a cloud, higher differential reflectivity values are caused by formation and/or growth of pristine ice crystal. This, however, does not explain observed anti-correlation between reflectivity and differential reflectivity.

3.1 Aggregation

In Figure 2 radio sounding measurements are shown for snowfall event that took place on March 3rd, 2009. These observations indicate presence of three cloud layers at around 300m, 2700m and from 5000m up. The lowest two layers appear to contain supercooled water.

In Figure 3 corresponding radar measurements are shown. It can be seen that high Z_{dr} layer is located at around 3km altitude. This is also the layer where the mean Doppler velocity, as measured by vertically pointing HYL radar, goes through a rapid change changes from 0.5 to 1 m/s. By comparing central and left panels in Figure 2, one can also see that higher Z_{dr} regions correspond to lower reflectivity values. If we zoom in and look just at one vertical

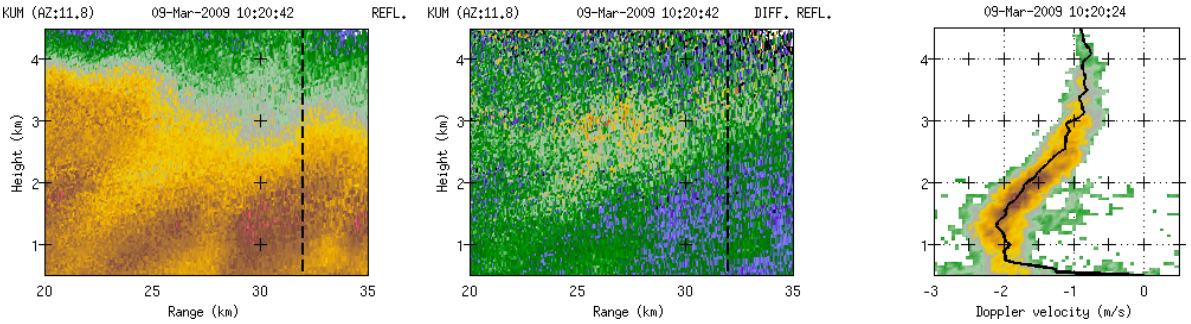

Figure 5 Same as Figure 3, only for measurements taken on March 9th, 2009 at 10.20 UTC

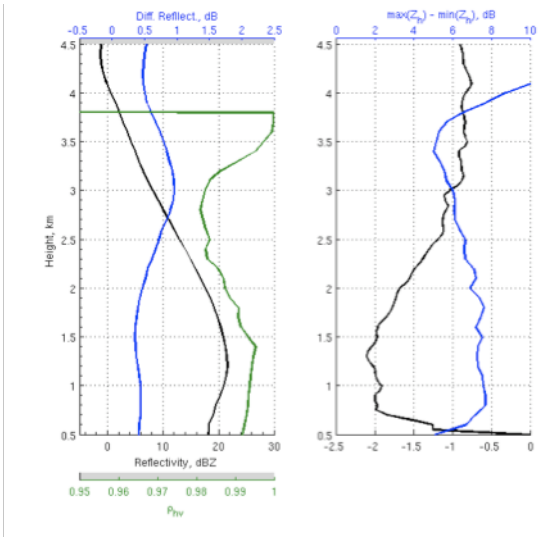

Figure 6 Same as Figure 4 only for the measurements shown in Figure 5.

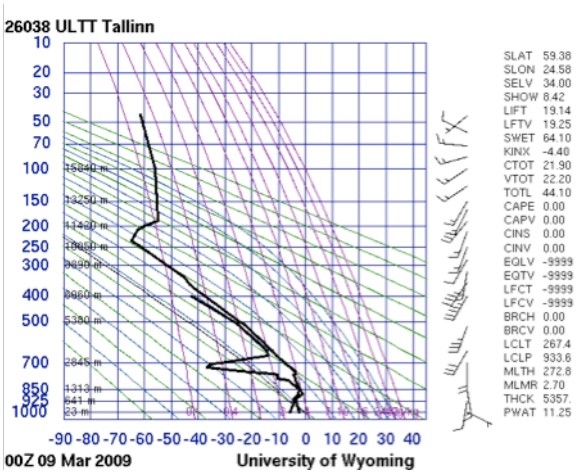

Figure 7 Sounding data for March 9th, 2009 case.

profile taken above HYL radar site, as shown in Figure 4, we will see that both Z_{dr} and reflectivity start to increase at about the same altitude. Then we can observe that the differential reflectivity starts to decrease as the mean Doppler velocity starts to increase.

Two snow growth processes take place in this layer. Due to presence of small amount of supercooled water, dendritic ice particles start to grow. Growth of these particles explains increase in Z_{dr} and initial increase in reflectivity. At the same time, these particles start to aggregate, that explains further increase in reflectivity and rapid change in the observed fall velocity. This aggregation pattern is very similar to the one observed by Lo and Pasarelli (1986).

Particle sorting most probably causes the apparent anti-correlation between Zdr and Ze. Aggregates have higher fall velocities than pristine crystals. Given the velocity differential, it takes around 200 s for pristine crystal and aggregates to separate by 100 m. We should note that due to the particle sorting the high Z_{dr} layer is self-maintaining and acts as a good indicator of aggregation.

In Figure 4 difference of maximum and minimum reflectivity values found in each height bin for the range interval of 29 to 35 km is plotted. This measurement acts as a good indicator of smoothness of the reflectivity field. It can be seen that there is hardly any dependence of the span of the reflectivity values on height. There is a slight preference for smaller values to be below 2 km. We will show that this measurement is useful for discrimination between aggregation and riming cases.

3.2 Riming

We have used vertically pointing Doppler radar to identify instances where riming was present. If one of the following two criteria was satisfied, we have concluded that riming is taking place. Firstly, we have assumed that riming is present if mean fall velocity of ice particles exceeded 1.7 m/s. Secondly, if we could detect a bimodal spectrum. Often, presence of a second mode also corresponded to a rapid increase in a mean fall velocity.

In Figure 5 measurements taken on March 9th, 2009 are shown. As can be seen from Doppler measurements riming is taking place. It can be observed from high fall velocities and apparent secondary spectral peak just below 2 km. The bimodality is most probably caused by secondary ice production. Similar to the pure aggregation case, this measurement also exhibits high Z_{dr} band cantered around 3 km height. As we have discussed above, this band is indication of deposition growth and aggregation of ice crystals. Riming is probably taking in height interval between 1 and 2 km.

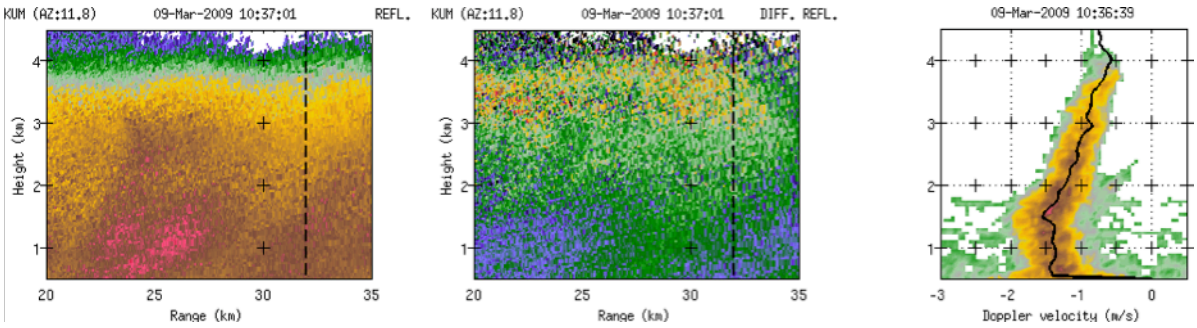

Figure 9 Same as Figure 6 only 17 min later.

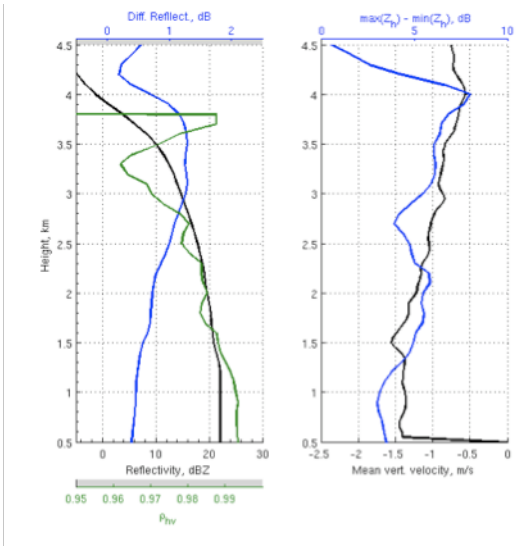

Figure 10 Vertical profiles of radar observables corresponding to Figure 9.

also shows a well-pronounced anti-correlation between reflectivity and differential reflectivity values. It is possible that this signature can also be attributed to particle sorting, where rimed particles precipitate out and secondary ice remains in the volume.

Given above described observations, it is not surprising to find that the span of reflectivity values, as shown in Figure 6, is higher for this measurement than one presented in Figure 4. It can be seen that not only the mean value is about 3-4 dB higher, but also the slope is different. If in the aggregation case the maximum difference between maximum and minimum reflectivity values is observed in the upper part of the curve, then for the riming case the higher values are located in the lower part of the curve. Or in other words, maximum reflectivity variability is observed in the areas where a dominating growth process is taking place.

It appears that variability of the reflectivity field is a useful parameter for discrimination between aggregation and riming processes.

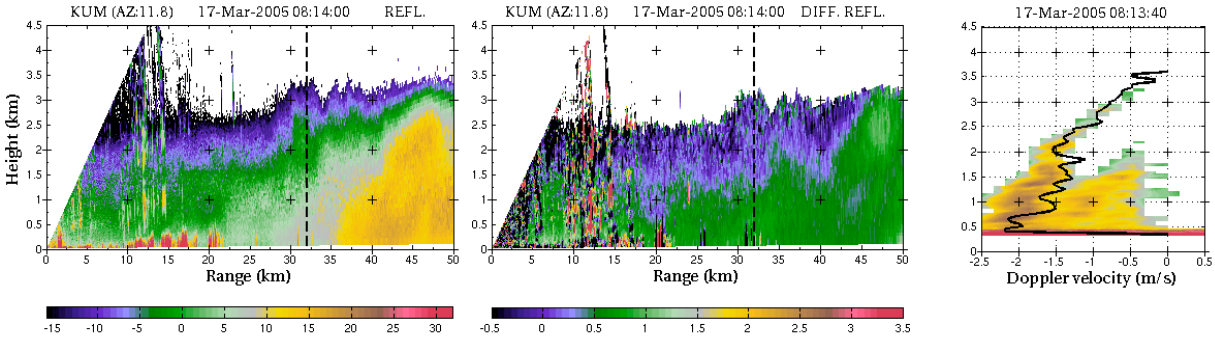

Figure 11. Observations of secondary ice generation on March 17th, 2005.

It is not clear whether increase in reflectivity below 2km height can be attributed to riming, or whether it is a continuation of aggregations process. In the left panel of Figure 5, one can see that reflectivity field exhibits more variability if compared to Figure 3. This feature is most probably related to the riming process. There are several possible explanations for this almost convective behaviour. Firstly, to form larger super cooled liquid droplets, which are needed for riming, the turbulent motion is required. Secondly, riming causes latent heat release that in its turn causes more air motion. Thirdly, this pattern

In Figure 9 and 10 radar observations that were taken 17 minutes after the ones presented above are shown. From Doppler measurements shown in Figure 9, one can see that mean Doppler velocities do not exceed 2 m/s, indicating light or no riming present. There is an apparent bimodality that can be seen in the height interval 1.5 -2.5 km. The remaining analysis of the Figures we are leaving to readers.

3.3 Intense secondary ice production

Secondary ice production is clearly observed during severe riming cases. Zawadzki et al (2001) have shown that in those cases a clearly identifiable secondary mode can be observed in Doppler spectral

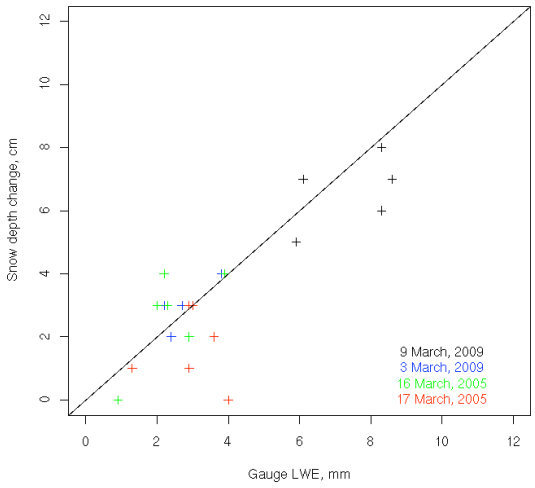

Figure 12. Accumulated 24 h precipitation (as liquid water equivalent, mm) and change in snow depth (in cm), 06-06 UTC at 5-7 weather stations within greater Helsinki area. Straight line represents the 1:10 density line.

measurements. Such an event took place on March 17th, 2005. It was observed that during this event there was no longer the anti-correlation between Z_{dr} and Z_e, as can be seen in Figure 11. This confirms that detected bimodality of Doppler spectra is due to secondary ice.

4. "SANITY" CHECK

Based on proposed above analysis, three snowfall events that took place in the greater Helsinki region were classified into whether they were dominated by aggregation or riming processes. It is not to say that during those events only one type of snow growth mechanism was present. This classification was done to identify events were riming was an observable phenomenon.

For this analysis we have selected snow events that took place on March 3rd, March 9th 2009, and March 17th 2005. For these days we have compared 24 h precipitation accumulations, as liquid water equivalent, and snow depth change within 24 h. These surface measurements were collected at 5-7 locations in the greater Helsinki area. The accumulations and snow depth changes are calculated for a time period from 6 UTC to 6 UTC. As a result, the snowstorm on March 17th 2005 was split into two parts. The snow storm has started around 0UTC on March 17th and has continued till late evening on the same day. This was a very fortunate split; since our analysis has indicated that before 6 UTC no (or very little) riming took place. After 6 UTC on the other hand, presence of heavy riming is indicated by the analysis.

From the other two cases, March 3rd 2009 is expected to have little or no riming and March 9th 2009 shows detectable riming signatures.

It is usually assumed that 1 mm of liquid water equivalent yields 1 cm of snow on the ground. This is based on assumption of snow density being equal to 0.1 g/cm^3.

In Figure 11 surface measurements during the selected snow events are shown. Straight line represents the 1:10 density line. Measurements above the line correspond to smaller density snowflakes, and measurements below the line correspond to denser, rimed particles.

5. CONCLUSIONS

It was demonstrated that morphological analysis of polarimetric measurements can be used to identify aggregation, riming, vapour deposition growth patterns as well as regions of intense secondary ice production. Based on comparison of polarimetric weather radar and vertically pointing Doppler radar observations patterns that correspond to different snow growth mechanisms were identified.

It was shown that a combination of reflectivity and differential reflectivity provides valuable information about underlying physical processes.

REFERENCES

Feng, D., and L. O. Grant, 1982: Correlation of snow crystal habit, number flux and snowfall intensity from ground observations. *Preprints, Conf. On Cloud Physics, Amer. Meteor. Soc.*, Boston, Massachusetts, 485-487.

Mitchell, D. L., R. Zhang and R. L. Pitter, 1990: Mass-dimensional relationships for ice particles and the influence of riming on snowfall rates., *J. Appl. Meteor.*, **29**, pp. 153-163.

Liu, H., and V. Chandrasekar, 2000: Classification of Hydrometeors Based on Polarimetric Radar Measurements: Development of Fuzzy Logic and Neuro-Fuzzy Systems, and In Situ Verification. *J. Atmos. Oceanic Technol.*, **17**, 140–164.

Straka, J.M., D.S. Zrnić, and A.V. Ryzhkov, 2000: Bulk Hydrometeor Classification and Quantification Using Polarimetric Radar Data: Synthesis of Relations. *J. Appl. Meteor.*, **39**, 1341–1372.

Lim, S., V. Chandrasekar, and V. N. Bringi, 2005: Hydrometeor classification system using dual-polarization radar measurements: Model improvements and in situ verification. *IEEE Trans. Geosci. Remote Sens.*, **43**, 792–801.

Zawadzki I., F. Fabry and W. Szymer, 2001: Observations of supercooled water and secondary ice generation by a vertically pointing X-band Doppler radar. *Atmos. Res.,* **59-60**, 343-359.

Lo K. K., and R. E. Passarelli, Jr., 1982: The growth of snow in winter storms: an airborne observational study. *J. Atmos. Sci., **39**,* 697-706

Hogan, R. J., P. R. Field, A. J. Illingworth, R. J. Cotton and T. W. Choularton, 2002: Properties of embedded convection in warm-frontal mixed-phase cloud from aircraft and polarimetric radar. *Quart. J. Roy. Meteorol. Soc.,* **128,** 451-476